International Journal of Robotics and Automation, Vol. 38, No. 10, 2023
An Open Access Paper

AN ADAPTIVE FORMULATION OF THE SMOOTH VARIABLE STRUCTURE FILTER BASED ON STATIC MULTIPLE MODELS

Andrew S. Lee,* S. Andrew Gadsden,** Stephen A. Wilkerson,*** and Mohammad AlShabi****

Abstract

The Kalman filter (KF) is the most well-known estimation strategy that yields the optimal solution to the linear quadratic estimation problem. The system in such applications shall be well modelled assuming the presence of Gaussian noise. While the KF is effective under the stated conditions, it lacks robustness to other types of disturbances. Therefore, numerous variants of the KF have been developed to accommodate its limitations. The smooth variable structure filter (SVSF) is an alternative solution with improved robustness, especially in the case of modelling uncertainties. It is based on a sliding-mode technique that offers robustness at the cost of optimality. On the other hand, some algorithms and solutions involve with several possible operating modes and generate an estimation based on the output of these models, *i.e.*, the static multiple models (SMMs) that obtain the estimates based on the weighted statistical fusing of the outputs of the models depending on the likelihood of each mode. This paper introduces an adaptive formulation of the SVSF that is reformulated based on SMMs. The proposed model is applied and tested on an electro-hydrostatic actuator (EHA). The proposed method takes the advantages of the SVSF's robustness and stability while reducing the estimation error due to the use of an adaptive modelling structure. The results show an improvement on the SVSF performance, where the root mean-squared errors are reduced by 41%, 99%, and 75% for the position, velocity, and acceleration estimated states. Therefore, the proposed method is a good candidate for parameter and state estimation problems.

Key Words

State and parameter estimation, Kalman filter, smooth variable structure filter, robustness, static multiple models

* Northrop Grumman, Baltimore, MD, USA; e-mail: alee32@uoguelph.ca
** Department of Mechanical Engineering, McMaster University, Hamilton, ON, Canada; e-mail: gadsden@mcmaster.ca
*** York College of Pennsylvania, York, PA, USA; e-mail: swilkerson@ycp.edu
**** Department of Mechanical and Nuclear Engineering, University of Sharjah, Sharjah, UAE; e-mail: malshabi@sharjah.ac.ae
Corresponding author: S. Andrew Gadsden

Recommended by Maki K. Habib
(DOI: 10.2316/J.2023.206-0879)

Table of Nomenclature

Symbols	Representation
$\circ$	Schur product.
X^+	Pseudoinverse of X.
X^{-1}	Inverse of X.
$\widehat{X}$	Estimated value of X.
$\|X\|$	Absolute value of X.
A	System matrix.
B	Input matrix.
C	Measurement matrix.
$X_{k\|k}$	The a posteriori value of X at time .
$X_{k\|k-1}$	The *a priori* value of X at time .
u_k	Input value at time k.
μ_k^j	Weight at time k for each model M^j.
σ_j^2	The variance of model $M^j M^j$.
sgn	Sign function.
n, m	Number of states and measurements, respectively.
γ	SVSF coefficient matrix.
ψ	Boundary layer vector.
z_k	Measurement value at time k.
P	Error covariance matrix.
Q	System noise's covariance matrix.
R	Measurement noise's covariance matrix.
x	State vector.
z	Measurement vector.
e_z	Error in measurement.
K_k	Correction gain at time k.
M^j	Model j structure.
T	The time step, 1 msec.
sat	Saturated function.
r	Number of models for SSM.
diag	Convert the vector to a diagonal matrix where the elements of the vector are the diagonal elements of the matrix.

1. Introduction

Estimating the dynamic behaviour involves the extraction of important values known as states from noisy measurements [1], [2]. States change over time and are typically governed by equations that describe system dynamics [3]. The estimation process is referred to as filter as it tries to minimise the noise effect. Most of the filters try to minimise the error (difference between the actual and estimated state values) while simultaneously reducing the effects of noise. The other types of filters try being robust to disturbances [3]. Disturbances and noise are typically present in measurements and may be caused by the sensor quality (system uncertainties) as well as environmental factors (measurement uncertainties). System uncertainties may be caused by an inaccurate model and/or variations and nonlinearities in the physical system parameters. Reliable estimates of state and/or parameters are necessary for safely and accurately controlling a system in real time. When system dynamics are changed abruptly in the presence of faults, adaptive estimation strategies that combined both types of filters can be used to mitigate inaccurate estimation. They maintain the stability of the filter during the fault while reducing the error in the estimation.

Kalman expanded on the research of his predecessors and introduced a new solution to linear filtering and tracking problems [4]. He derived a filter that utilized linear models and measurements to yield an optimal estimation based on strict assumptions. This filter later became known as the Kalman filter (KF). As the KF is applicable to linear Gaussian models, several works were conducted to modify the KF and make more applicable to nonlinear and/or non-Gaussian models, *i.e.*, extended KF and unscented KF [4].

Another branch of estimation methods is still developing in parallel to the KF and its variants. This branch includes the well-known sliding-mode observers (SMOs). These observers are based on variable structure (VS) and sliding-mode (SM) techniques [5]–[7]. Both techniques consider the system has discontinuity in its structure. Therefore, they define discontinuation hyperplanes that divide the state space into different regions; within these regions, the equations used to describe the system are continuous [8], [9]. The name "VS" is chosen because system dynamics may be mathematically described by a finite number of equations.

VS theory provided the foundation for VS control (VSC). In VSC, the controller signal is formulated as a discontinuous state function, such that discontinuity hyperplanes are introduced [8], [9]. The most well-known type of VSC is the SM controller (SMC) [6], [10]. SMC makes use of a discontinuous switching plane along a desired state trajectory, which is referred to as the sliding surface. The primary objective for the SMC is to maintain the states within sliding surface neighbourhood. A switching gain is used to push the states towards the surface when they try to move away. Once the state values are on the surface, the states slide along the surface towards the desired values [10]. Although the switching effects bring robustness and stability to the control process, it also introduces high-frequency switching known as chattering [11]. Quite often a boundary layer is introduced in an effort to smooth out the control signal [10]. Prior to the 1980s, VSC and SMC methods were only considered in the continuous-time domain [12]. In 1985, a discrete-time formulation of SMC was presented [13]. A stability condition was provided shortly afterwards and is now typically used in the design of discrete controllers [14], [15].

SMOs, which were developed in the 1980s [12], [16], reduce the error with the help of a switching function similar to VSC and SMC [17]. Observer gains are calculated based on the errors between the measurements and estimates [17]. Most SMOs apply a discontinuous signal to the estimates in order to keep them bounded to an area of the surface [12]. The motion consists of three phases: reachability, injection, and sliding [12], [18]. The reachability phase consists of forcing the estimates to the sliding surface from some initial conditions, in a finite period of time [12]. Once within a defined area of the surface (called an existence subspace), both the injection and sliding phases are present. The sliding phase forces the estimated errors to slide along a hyperplane towards the origin [12]. The injection phase consists of preventing the estimate from leaving the existence subspace; keeping it bounded within an area of the sliding surface [12]. According to [12], [16], and [19], the action of the injection phase enables the observer to be robust enough to overcome uncertainties, modelling errors, and nonlinearities present in the system. A number of SMOs have been developed based on these principles. The most notable observers were introduced by Slotine *et al.* [9], [20], Walcott *et al.* [21], [22], Edwards and Spurgeon [19], and later by both Tan and Edwards [23]. SMOs have been applied to estimation problems, and fault detection and isolation [12].

Another filter called the smooth VS filter (SVSF) was presented in 2007, which was based on SM and VS techniques [3], [12], [24]. The SVSF is formulated as a predictor–corrector estimator similar to the KF. However, it utilises a gain structure based on SM techniques. The filter's gain is calculated based on the error in measurements at the prediction stage of the current time (known as innovation), the error in measurements at the update stage from the previous time step, and a switching term [24]. Similar to SMOs, the switching gain structure improves the stability and robustness of the estimation process by bounding the state estimates close to the true trajectory [25], [26]. The SVSF presented in [24] did not contain a state error covariance derivation, which is an important feature for optimal estimation strategies (it is another performance indicator). A state error covariance function was introduced and expanded in [25], [27], and [28], which vastly improved the number of useful applications for the SVSF [29]–[31]. Other developments and improvements to the SVSF were conducted in the literature, including fault detection using chattering, higher-order implementations, and tracking multiple targets [12], [32]–[35]. The SVSF has demonstrated robust performance on a number of different estimation problems [4]. Most recently, a filter, which is referred to as the sliding innovation filter (SIF), was introduced in [36]–[39]. The SIF is based on similar concepts to the SVSF but offers a simpler formulation with improved results. An opportunity for improving the SVSF involves the development of an adaptive formulation. The ability of the SVSF to automatically modify its system and/or measurement models based on different operating modes offers significant room for improvement (*e.g.*, in terms of both accuracy and robustness).

In this paper, a new adaptive formulation of the SVSF is presented and tested on an experimental setup. The novel method integrates the static multiple models (SMMs) estimator with the SVSF predictor–corrector estimation strategy. The SMM consists of several possible operating modes where several possible estimates are obtained. The SMM then combines these estimates using some weights based on the likelihood of each mode. This strategy may be used for fault detection and diagnosis problems and has demonstrated good accuracy and repeatability of results. The performance of the proposed method is evaluated using an electro-hydrostatic actuator (EHA) which was built for experimentation. The results are compared with the standard SVSF estimation method.

This paper is organised as follows. Section 2 summarises the SVSF estimation process. Section 3 introduces the SMM estimator and the proposed SMM-SVSF or the adaptive SVSF algorithm. Section 4 describes the experimental setup as well as the equations of motion governing the EHA. Section 5 discusses the application of the standard SVSF and adaptive SVSF to the EHA system, followed by concluding remarks.

2. The Smooth Variable Structure Filter

The SVSF is a predictor–corrector estimation strategy that offers solution with robustness and stability against disturbances and uncertainties. The SVSF uses a smoothing boundary layer with an upper bound that is defined based on the level of noise and unmodeled dynamics [40], [41]. The SVSF is model-based and may be applied to both linear or nonlinear systems and measurements [3], [12]. The SVSF's concepts are illustrated in Fig. 1.

As described earlier, the SVSF strategy is structured similarly to the KF. However, it presents a novel way to calculate its gain. As per (2.1) and (2.2), $\widehat{x}_{k+1|k}$ and $P_{k+1|k}$ are calculated.

$$\widehat{x}_{k+1|k} = A\widehat{x}_{k|k} + Bu_k \tag{2.1}$$
$$P_{k+1|k} = AP_{k|k}A^T + Q_k \tag{2.2}$$

Then, $\widehat{z}_{k+1|k}$ and $e_{z,k+1|k}$ are calculated as per (2.3) and (2.4), respectively.

$$\widehat{z}_{k+1|k} = C\widehat{x}_{k+1|k} \tag{2.3}$$
$$e_{z,k+1|k} = z_{k+1} - \widehat{z}_{k+1|k} \tag{2.4}$$

The gain used by the SVSF, K_k, is calculated with the use of the boundary layer widths, ψ, as follows [3]:

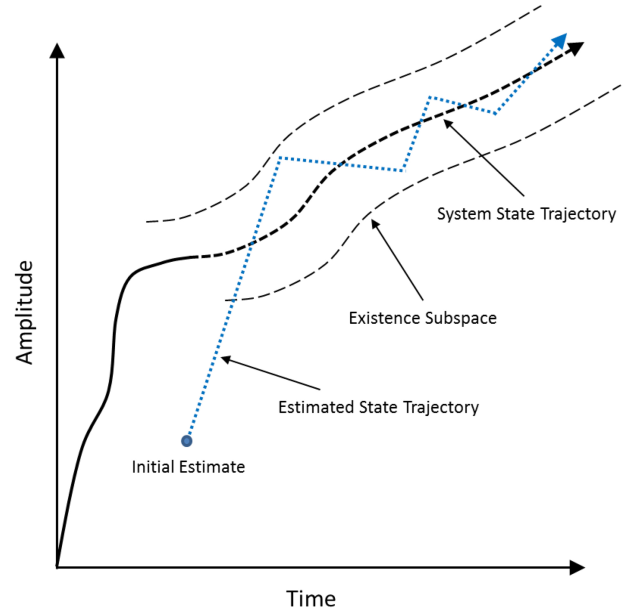

Figure 1. SVS's concepts with the existence subspace boundary layer [3].

$$K_{k+1} = C_k^+ \operatorname{diag}\left[\left(\left|e_{z_{k+1|k}}\right| + \gamma\left|e_{z_{k|k}}\right|\right) \circ \operatorname{sat}\left(\overline{\psi}^{-1} e_{z_{k+1|k}}\right)\right] \operatorname{diag}\left(e_{z_{k+1|k}}\right)^{-1} \tag{2.5}$$

The saturation function is defined as follows:

$$\operatorname{sat}\left(\overline{\psi}^{-1} e_{z_{k+1|k}}\right) = \begin{cases} 1, & e_{z_i,k+1|k}/\psi_i \geq 1 \\ \frac{e_{z_i,k+1|k}}{\psi_i}, & -1 < \frac{e_{z_i,k+1|k}}{\psi_i} < 1 \\ -1, & e_{z_i,k+1|k}/\psi_i \leq -1 \end{cases} \tag{2.6}$$

where $\overline{\psi}^{-1}$ is defined by (2.7) for m number of measurements [3]:

$$\overline{\psi}^{-1} = \begin{bmatrix} \frac{1}{\psi_1} & 0 & 0 \\ 0 & \ddots & 0 \\ 0 & 0 & \frac{1}{\psi_m} \end{bmatrix} \tag{2.7}$$

The state vector and error covariance matrix are, respectively, updated as per (2.8) and (2.9).

$$\widehat{x}_{k+1|k+1} = \widehat{x}_{k+1|k} + K_{k+1}e_{z,k+1|k} \tag{2.8}$$
$$P_{k+1|k+1} = \left(I - K_{k+1}C\right)P_{k+1|k}\left(I - K_{k+1}C\right)^T + K_{k+1}R_{k+1}K_{k+1}^T \tag{2.9}$$

Finally, the updated measurement error, $e_{z,k+1|k+1}$, is found as per (2.10) and is used in the next iteration.

$$e_{z,k+1|k+1} = z_{k+1} - \widehat{z}_{k+1|k+1} \tag{2.10}$$

The existence subspace, denoted by the dotted black line shown in Fig. 1, refers to the level of uncertainty found in the estimation process. It is typically present due to the amount of noise and/or modelling uncertainties [3]. The existence space, β, is described mainly from the innovation signal [27], [34]. While the width is not precisely known,

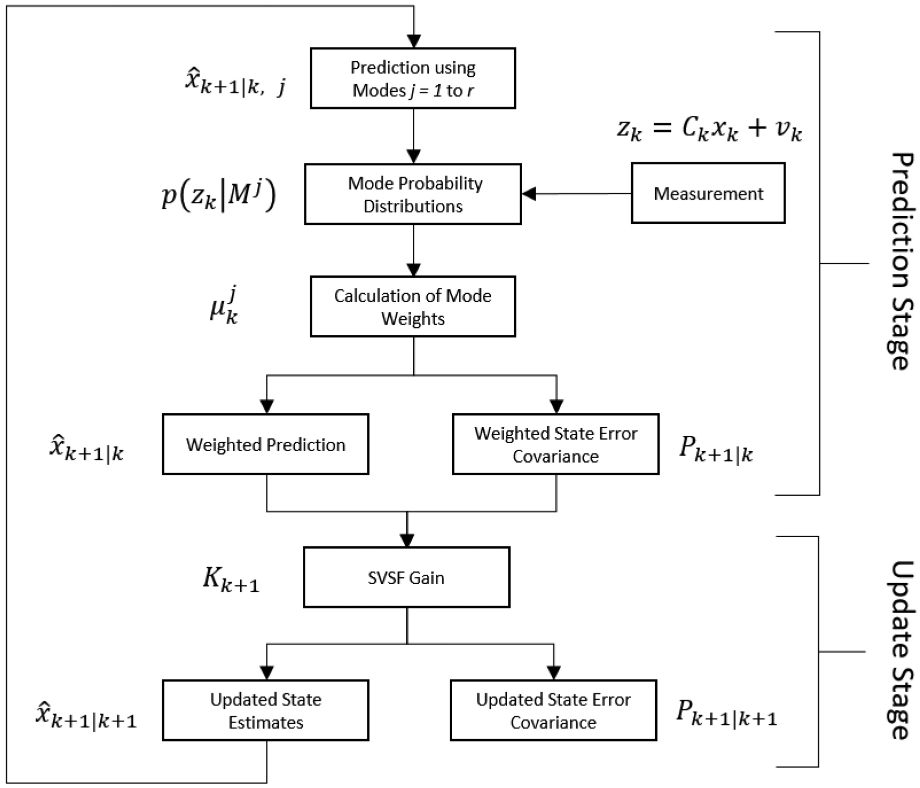

Figure 2. The proposed SMM-SVSF (or adaptive SVSF) flowchart.

designer knowledge may be used to define the upper bound. When the smoothing boundary is defined larger than the existence subspace, the estimated states are smoothed. Likewise, if the smoothing term is set too small, chattering (high-frequency switching) may occur.

3. A Novel Adaptive Formulation of the Smooth Variable Structure Filter

The SMM algorithm assumes that the system behaves according to a finite number of r models $M^1, M^2, \ldots, M^r$. The SMM uses variable weights, μ_k^j, calculated at time k to represent each model M^j. These weights represent a probability of the system behaving according to a corresponding operating mode (*i.e.*, mathematical model). These weights are used to combine the corresponding model state estimates [42] which creates an overall estimate. The weights are initially uniformly distributed, and subsequent weights are calculated as follows:

$$\mu_k^j = \frac{p\left(z_k \middle| M^j\right) \mu_{k-1}^j}{\sum_{i=1}^r p\left(z_k \middle| M^i\right) \mu_{k-1}^i} \tag{3.1}$$

where $p\left(z_k \middle| M^j\right)$ is the likelihood value of measurement z_k based on M^j and is defined as follows:

$$p\left(z_k \middle| M^j\right) = \frac{1}{\sqrt{2\pi\sigma_j^2}} \exp \frac{-\left(z_k - \widehat{z}_{k|k-1}\right)^2}{2\sigma_j^2} \tag{3.2}$$

$$\sigma_j^2 = C_k^j P_{k|k-1}^j {C_k^j}^T + \left(\sigma_z^2\right)^j \tag{3.3}$$

where σ_j^2 refers to the variance of model M^j based on the predicted measurement $\widehat{z}_{k|k-1}$ for model M^j [42]. Note that the parameter definitions may also be found in the Table of Nomenclature. Each model has its own likelihood value calculated from the filtering strategy (whether it is from a KF, SVSF, or another type). The adaptive estimates are calculated using the weighted sum produced by the system models, as per (3.4).

$$\widehat{x}_{k|k} = \sum_{j=1}^r \mu_k^j \widehat{x}_{k|k}^j \tag{3.4}$$

The adaptive covariance is calculated in a similar fashion, as shown in (3.5).

$$P_{k|k} = \sum_{j=1}^r \mu_k^j \left[P_{k|k}^j + \left(\widehat{x}_{k|k}^j - \widehat{x}_{k|k}\right)\left(\widehat{x}_{k|k}^j - \widehat{x}_{k|k}\right)^T\right] \tag{3.5}$$

The proposed SMM-SVSF (or adaptive SVSF) uses the model weights from the SMMs estimator to generate a weighted prediction. The weighted state predictions are used to calculate the SVSF gain, which is used to generate an updated state estimate and state error covariance. As the algorithm uses a weighted combination of system modes, the weights could be used to describe the mixing of different system modes. Figure 2 depicts the algorithm flowchart and Table 1 shows the corresponding pseudocode. Note that the initial mode weights can be defined by the user, provided that the sum of each value is 1 (so the total probability is 100%).

After the SVSF boundary layer vector and convergence rate have been set and model weights have been initialised,

Table 1
Pseudocode for the SMM-SVSF Algorithm

1:	For models (M^j), $j = 1$ to r
	$\widehat{x}_{k+1\|k,\ \_j} \leftarrow (A_j, u)$
2:	For models (M^j), $j = 1$ to r
	$\sigma \leftarrow (Q,\ R,\ P_{k\|k})$
	$p \leftarrow (\widehat{x}_{k+1\|k,\ j},\ z,\ \sigma)$
3:	$\mu_{k+1} \leftarrow (\widehat{x}_{k+1\|k,j},\ \mu_k)$
4a:	$\widehat{x}_{k+1\|k} \leftarrow (\widehat{x}_{k+1\|k,\ j},\ \mu_{k+1})$
4b:	For operating modes $j = 1$ to r
	$P_{k+1\|k,j} \leftarrow (A_j,\ \widehat{x}_{k+1\|k})$
5:	$P_{k+1\|k} \leftarrow (P_{k+1\|k,j},\ \mu_{k+1})$
6:	$K_{k+1} \leftarrow (C, \gamma, \text{saturation})$
7a:	$\widehat{x}_{k+1\|k+1} \leftarrow (\widehat{x}_{k+1\|k,},\ z,\ C,\ K_{k+1})$
7b:	$P_{k+1\|k+1} \leftarrow (P_{k+1\|k},\ C,\ K_{k+1},\ R)$

a predicted state estimate for each system model is made. The standard deviation is calculated using three different covariance matrices: the state error, the system noise, and the measurement noise covariance matrices. Next, the updated estimates, standard deviations, and measurements are used to calculate the model probabilities. These probabilities are then used to update the model weights, which then are used to generate a weighted predicted state estimate and error covariance. This information is fed through the SVSF update stage as described in Section 2 using (2.8)–(2.10).

4. Experimental Setup

EHAs are a type of hydraulic and electrical actuator comprised of a linear or rotary actuator, a hydraulic circuit, and a bidirectional pump [43]. EHAs are used in automotive and aerospace industry due to their large force-to-weight ratios and their reliability. They are also used in various manufacturing applications, such as metal forming, where control of the outlet pressure is required [44]. Electromechanical systems often function under different operating modes. In the case of the EHAs, faults, such as internal leakage and increased friction, may be present. Internal leakage is caused by the wearing of the piston seal, which affects the overall actuation performance [45]. If the leakage remains undetected, then it cannot be repaired, which can deteriorate lifetime performance and increase maintenance costs [45]. As detection of internal leakage in EHAs through disassembly of the cylinder and piston is costly, adaptive estimation strategies can be used to improve the overall estimation process in the presence of multiple operating modes.

The EHA model used in this paper was designed and manufactured at the Centre for Mechatronics and Hybrid Technology at McMaster University shown in Fig. 3 [43]. The EHA used in this study is composed of several components, including two linear actuators, a bi-directional external gear pump, a variable-speed servomotor, an accumulator, a pressure relief valve, and safety circuits [46]. A variable-speed brushless DC electric motor drives the pump and forces hydraulic oil into the cylinder and modifies the actuation performance by varying the fluid flow rate. An accumulator is used to prevent cavitation and collect leakages from the gear pump. The EHA is controlled by modifying the input voltage to the motor, which consequently changes the direction and speed of the pump. Controlling the fluid flow rate in the outer circuit adjusts the position of the piston, which could be used for aerospace applications such as changing flight surfaces.

The EHA was modelled using four states: the actuator position $x_1 = x$, velocity $x_2 = \dot{x}$, acceleration $x_3 = \ddot{x}$, and differential pressure across the actuator $x_4 = P_1 - P_2$. The physical modelling approach was used to obtain the nonlinear state-space equations in discrete time described by [3], [47]:

$$x_{1,k+1} = x_{1,k} + T x_{2,k} \tag{4.1}$$

$$x_{2,k+1} = x_{2,k} + T x_{3,k} \tag{4.2}$$

$$\begin{aligned} x_{3,k+1} = {} & 1 - \left[T \frac{a_2 V_0 + M \beta_e L}{M V_0} \right] x_{3,k} \\ & - T \frac{\left({A_E}^2 + a_2 L \right) \beta_e}{M V_0} x_{2,k} \cdots \\ & - T \frac{2 a_1 V_0 x_{2,k} x_{3,k} + \beta_e L \left(a_1 {x_{2,k}}^2 + a_3 \right)}{M V_0} \operatorname{sgn}\left(x_{2,k} \right) \\ & + T \frac{A_E \beta_e}{M V_0} u \end{aligned} \tag{4.3}$$

$$x_{4,k+1} = \frac{a_2}{A_E} x_{2,k} + \frac{\left(a_1 {x_{2,k}}^2 + a_3 \right)}{A_E} \operatorname{sgn}\left(x_{2,k} \right) + \frac{M}{A_E} x_{3,k} \tag{4.4}$$

The system input is defined as follows:

$$u = D_p \omega_p - \operatorname{sgn}\left(P_1 - P_2 \right) Q_{L0} \tag{4.5}$$

where ω_p is the pump speed. Table 2 summarises and defines the numeric values of the parameters in (4.1)–(4.5).

The friction was modelled using a quadratic function based on the actuator velocity. The friction coefficients were obtained by performing experiments ranging from 15.6 to 109 radians per second with each data set containing four trials for repeatability [43].

5. Results and Discussion

The results of applying the proposed strategy on the EHA are discussed in this section. The state estimates were initialised to zero and the covariance matrices for system and measurement noises were defined, respectively, as $Q = 10^{-9} I_{4x4}$ and $R = 10^{-6} I_{4x4}$, where I is an identity matrix. Furthermore, the state error covariance matrix P was initialised as $10Q$.

Leakage faults were introduced to investigate the effects of parametric uncertainties in the system. The purpose of this study was to demonstrate the efficiency of the proposed strategy compared to the standard SVSF. The SMM-SVSF algorithm demonstrates robustness in the

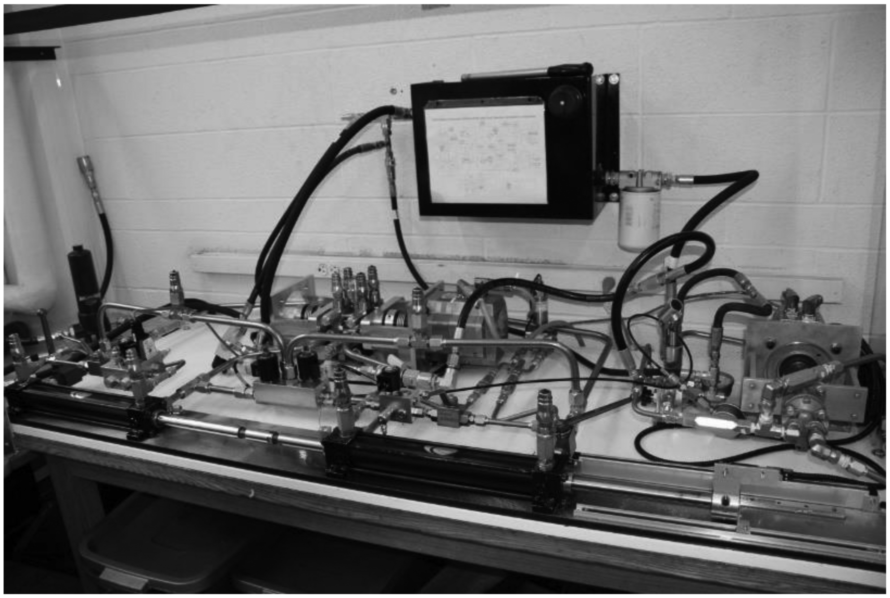

Figure 3. Prototype of the EHA used to collect experimental data [43].

Table 2
The EHA Parameters, Definitions, and Values Used in the Experiment

Parameter	Description	Parameter Values
A_E	Piston area (m^2)	1.52×10^{-3}
D_p	Pump displacement (m^3/rad)	5.57×10^{-7}
L	Leakage coefficient (m^3/(s×Pa))	4.78×10^{-12}
M	Load mass (kg)	7.376 kg
Q_{L0}	Flow rate offset (m^3/s)	2.41×10^{-6}
V_0	Initial cylinder volume (m^3)	1.08×10^{-3}
β_e	Effective bulk modulus (Pa)	2.07×10^{8}
a_1	Friction coefficient	6.589×10^{4}
a_2	Friction coefficient	2.144×10^{3}
a_3	Friction coefficient	436

Table 3
Leakage Coefficient Values and Flow Rate Offsets for Varying Operating Conditions

Condition	Leakage, L (m^3/(s×Pa))	Flow Rate Offset, Q_{L0} (m^3/s)
Normal	4.78×10^{-12}	2.41×10^{-6}
Minor leakage	2.52×10^{-11}	1.38×10^{-5}
Major leakage	6.01×10^{-11}	1.47×10^{-5}

presence of multiple operating modes. Multiple system modes are introduced to the system in the form of leakage faults. In order to obtain the coefficients of the leakage values, the EHA was operated with a constant pump speed of 94.25 radians per second under a series of differential pressures. The differential pressure was modified using a throttling valve in the hydraulic system. To ensure repeatability, five sets of measurements were made. A linear regression was performed on each data set, and the slope and intercept were used to define L and Q_{L0}, respectively. The leakage coefficients and flow rate offsets used for this study are presented in Table 3.

A minor leakage is introduced to the system at $t = 3$ sec and a major leakage is introduced at $t = 6$ sec. The effect on the input flow rate can be seen in Fig. 4.

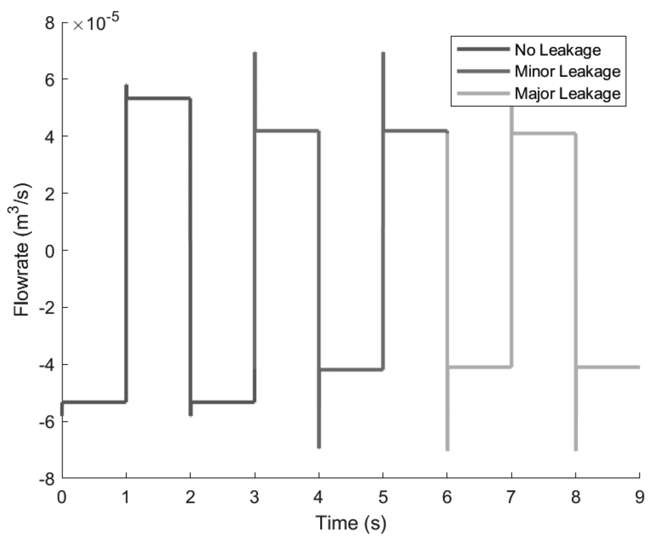

Figure 4. Input flow rate due to internal leakage faults.

Once the EHA was modelled at all these operations and they were verified experimentally, we used these mathematical models and values in a MATLAB Simulation to compare the performance between the proposed algorithm to the traditional one. The benefits of using the

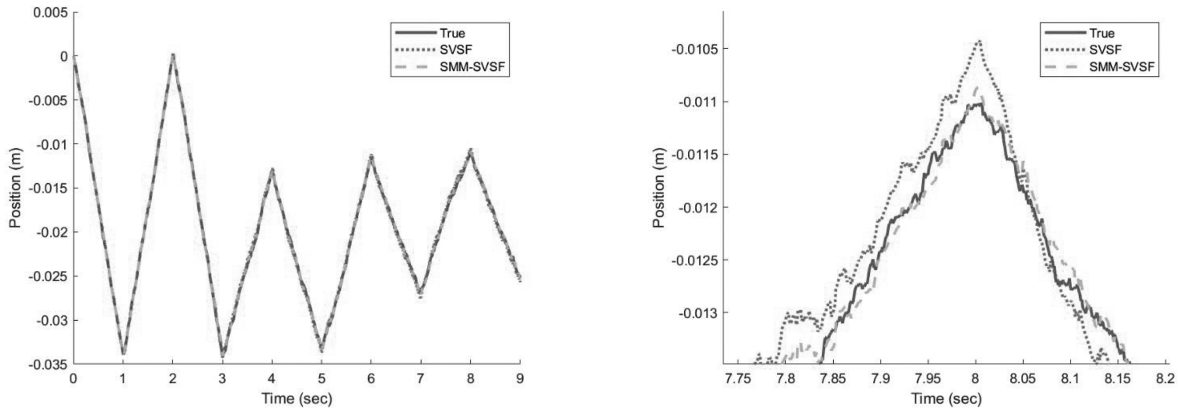

(a) (b)

Figure 5. Position estimates with leakage faults: (a) 9-sec simulation and (b) zoomed in at 8 sec (major leakage).

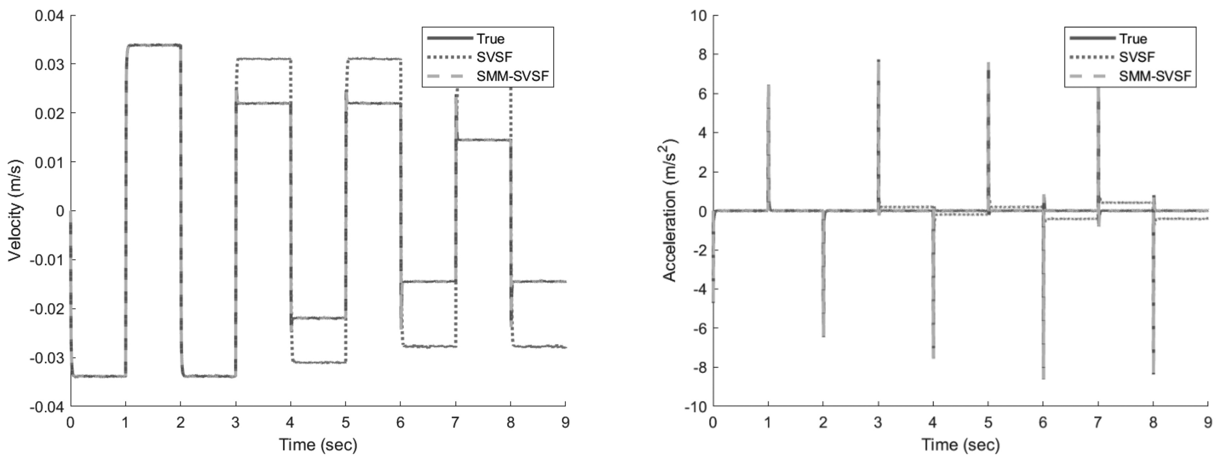

(a) (b)

Figure 6. (a) Velocity estimates for EHA with leakage faults and (b) acceleration estimates with leakage faults.

simulation can be summarised in two points; the values at a certain point are known, *i.e.*, the true state, and the prototype will not be damaged due to the fault when introduced. The results of the simulation are shown in Figs. 5–8 and Table 4.

Figure 5 shows the position estimates, while the velocity and acceleration estimates are shown in Fig. 6(a) and 6(b), respectively. The SMM-SVSF performs slightly better than the classical SVSF when the major leakage fault is introduced as seen in Fig. 5(a) and (b). The SVSF filter shows a significant deviation from the true velocity when the minor leakage fault is introduced at 3 sec, as shown in Fig. 6(a). The error becomes worse when the major leakage is introduced at 6 sec as shown in Fig. 6(b). This error is caused by the modelling uncertainty of the acceleration state, particularly due to the flow rate offset of the input. The greatest improvement can be seen in the velocity and acceleration estimates. Overall, the SMM-SVSF greatly outperforms the classical SVSF in the presence of modelling uncertainties such as leakage faults.

The SMM-SVSF's ability to determine system modes can be seen in Fig. 7, which shows the weights of each system mode used to calculate the estimate. Throughout

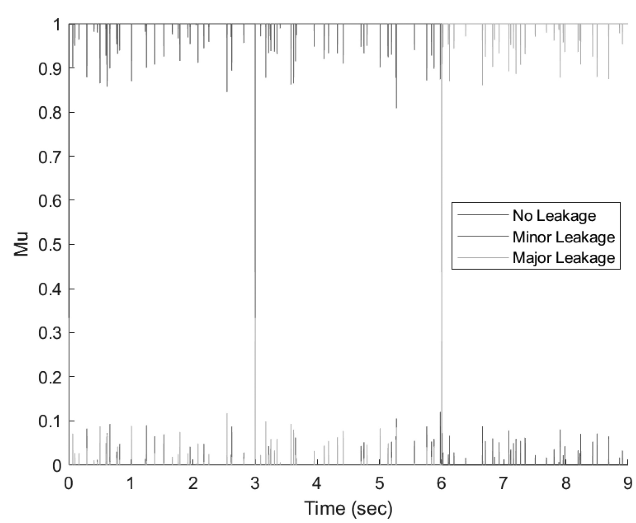

Figure 7. Model probability weights.

the entire experiment, the SMM-SVSF filter calculates at least an 80% probability of the correct operating mode at every stage of operation. The figure shows clear transitions from normal operation, to minor leakage, to major leakage

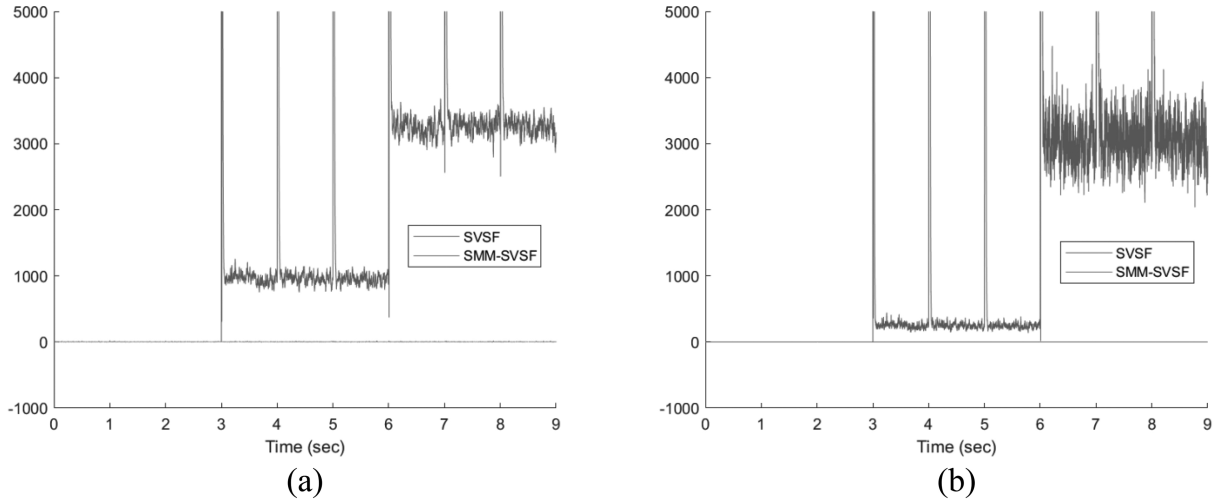

Figure 8. The differences between SVSF and SMM-SVSF in terms of (a) IS and (b) ES.

Table 4
RMSE Results for SVSF and SMM-SVSF for Scenario With Leakage Faults

Filter	Position (m)	Velocity (m/s)	Acceleration Acceleration	Differential Pressure (Pa)
SVSF	0.0003101	0.0091966	0.002810	0.001002
SMM-SVSF	0.0001828	0.0000799	0.000712	0.001002

at 3 and 6 sec, respectively. The innovation squared (IS) and error squared (ES) are calculated and shown in Fig. 8. These two compare the *a priori* and the *a posteriori* squared errors between the two algorithms, respectively. Moreover, they show the existence subspaces around the estimates in both prediction and update steps. From the figure, it was easily obtained that the SMM-SVSF is more stable compared to the classical SVSF, and estimates are smoother with no chattering in SMM-SVSF compared to SVSF. The error of the classical SVSF in both steps increases due to introducing the faults, and it spikes when the actuator changes direction. In addition, the RMSE values in Table 4 show that the SMM-SVSF significantly reduces the errors in estimating the position, velocity, and acceleration.

6. Conclusion

This paper introduced the combination of the SVSF and SMM estimation strategies to create an adaptive filtering method, SMM-SVSF, that can be used in fault and diagnosis applications. Furthermore, a brief background was provided on the development of estimation theory, up to and including the SIF. The SVSF was also included. The SMM-SVSF was tested on an EHA. The filter performed well for this particular EHA model due to two main factors: the system parameters of the different leakage modes vary significantly enough for mode differentiation using the SMM method, and the system and measurement noise covariances are well known. This paper demonstrates that the addition of SMM to the SVSF strategy improves the overall estimation process for a system with multiple operating modes, and thereby creates an adaptive SVSF. This can be observed from the results, where the root mean-squared errors were reduced by 41%, 99%, and 75% for the position, velocity, and acceleration estimated states when the SMM-SVSF is applied rather than SVSF. Potential future work will incorporate additional operating modes, such as friction faults as well as the mixing of several different operating modes.

References

[1] B. Ristic, S. Arulampalam, and N. Gordon, *Beyond the Kalman filter: Particle filters for tracking applications.* (Boston, MA: Artech House, 2004).

[2] M. Avzayesh, M. Abdel-Hafez, M. AlShabi, and S.A. Gadsden, The smooth variable structure filter: A comprehensive review, *Digital Signal Processing*, *110*, 2021, 102912.

[3] S.A. Gadsden, *Smooth variable structure filtering: Theory and applications.* (Hamilton, ON: McMaster University, 2011).

[4] H.H. Afshari, S.A. Gadsden, and S.R. Habibi, Gaussian filters for parameter and state estimation: A review of theory and recent trends, *Signal Processing*, *135*, 2017, 218–238.

[5] V.I. Utkin, Variable structure systems with sliding modes, *IEEE Transactions on Automatic Control*, *22*(2), 1977, 212–222.

[6] V.I. Utkin, *Sliding mode and their application in variable structure systems.* (Moscow: Mir Publ., 1978).

[7] A.F. Fillipov, *Differential equation with discontinuous right hand side, 62.* Providence, RI: American Mathematical Society Transactions, 1969.

[8] V.I. Utkin, *Sliding modes in control optimization.* (New York, NY: Springer-Verlag, 1992).

[9] J.J.E. Slotine, J. Hedrick, and E. Misawa, On sliding observers for nonlinear systems, *ASME Journal of Dynamic Systems, Measurement and Control*, *109*(3), 1987, 245–252.

[10] J.J.E. Slotine and W. Li, *Applied nonlinear control.* (Englewood Cliffs, NJ: Prentice-Hall, 1991).

[11] S.A. Gadsden and A.S. Lee, Advances of the smooth variable structure filter: Square-root and two-pass formulations, *Journal of Applied Remote Sensing*, *11*(1), 2017, 1–19.

[12] M. Al-Shabi, *The general toeplitz/observability SVSF.* (Hamilton, ON: McMaster University, 2011).

[13] C. Milosavlejic, General conditions for the existence of a quasi-sliding mode on the switching hyperplane in discrete variable structure systems, *Automatic Remote Control*, *46*, 1985, 307–315.

[14] K. Furuta, Sliding mode control of a discrete system, *Systems Control Letters*, *14*, 1990, 145–152.

[15] S.Z. Sarpturk, Y. Istefanopoulos, and O. Kaynak, On the stability of discrete-time sliding mode control systems, *IEEE Transactions on Automatic Control*, *AC-32*(10), 1987, 930–932.

[16] S.K. Spurgeon, Sliding mode observers: A survey, *International Journal of Systems Science*, *39*(8), 2008, 751–764.

[17] S.H. Qaiser, A.I. Bhatti, M. Iqbal, R. Samar, and J. Qadir, Estimation of precursor concentration in a research reactor by using second order sliding mode observer, *Nuclear Engineering and Design*, *239*, 2009, 2134–2140.

[18] S.H. Qaiser, A.I. Bhatti, R. Samar, M. Iqbal, and J. Qadir, Higher order sliding mode observer based estimation of precursor concentration in a research reactor, *Proc. 4th IEEE Conf. on Emerging Technologies*, Rawalpindi, 2008, 338–343.

[19] C. Edwards and S. Spurgeon, On the development of discontinuous observers, *International Journal of Control*, *59*, 1994, 1211–1229.

[20] J.-J.E. Slotine, J.K. Hedrick, and E.A. Misawa, On sliding observers for nonlinear systems, *Proc. American Control Conf.*, Seattle, WA, 1986, 1794–1800.

[21] B. Walcott and S. Zak, State observation of nonlinear uncertain dynamical systems, *IEEE Transactions on Automatic Control*, *AC-32*(2), 1987, 166–170.

[22] B. Walcott, M. Corless, and S. Zak, Comparative study of state observation techniques, *International Journal of Control, 45*(6), 1987, 2109–2132.

[23] C. Tan and C. Edwards, Sliding mode observers for robust detection and reconstruction of actuator and sensor faults, *International Journal of Robust and Nonlinear Control*, *13*(1), 2003, 443–463.

[24] S.R. Habibi, The smooth variable structure filter, *Proceedings of the IEEE*, *95*(5), 2007, 1026–1059.

[25] S.A. Gadsden, *Smooth variable structure filtering: Theory and applications*, PhD Thesis, McMaster University, Hamilton, ON, Canada, 2011.

[26] S.A. Gadsden, S.R. Habibi, and T. Kirubarajan, Kalman and smooth variable structure filters for robust estimation, *IEEE Transactions on Aerospace and Electronic Systems*, *50*(2), 2014, 1038–1050.

[27] S.A. Gadsden, M. El Sayed, and S.R. Habibi, Derivation of an optimal boundary layer width for the smooth variable structure filter, *Proc. ASME/IEEE American Control Conf. (ACC)*, San Francisco, CA, 2011, 4922–4927.

[28] S.A. Gadsden and S.R. Habibi, A new robust filtering strategy for linear systems, *ASME Journal of Dynamic Systems, Measurement, and Control*, *135*(1), 2013, 9.

[29] S.A. Gadsden, M. Al-Shabi, and S.R. Habibi, Estimation strategies for the condition monitoring of a battery system in a hybrid electric vehicle, *ISRN Signal Processing*, *2011,* 2011, 120351.

[30] J. Goodman, J. Kim, A.S. Lee, and S.A. Gadsden, A variable structure-based estimation strategy applied to an RRR robot system, *Journal of Robotics, Networking and Artificial Life*, *4*(2), 2017, 142–145.

[31] J. Kim, S. Bonadies, C.D. Eggleton, and S.A. Gadsden, Cooperative robot exploration strategy using an efficient backtracking method for multiple robots, *ASME Journal of Mechanisms and Robotics*, *10*(6), 2018, 7.

[32] M. Al-Shabi, S.A. Gadsden, and S.R. Habibi, Kalman filtering strategies utilizing the chattering effects of the smooth variable structure filter, *Signal Processing*, *93*(2), 2013, 420–431.

[33] H.H. Afshari, *The 2nd-order smooth variable structure filter (2nd-SVSF) for state estimation: Theory and applications*, PhD Thesis, McMaster University, Hamilton, ON, Canada, 2014.

[34] S.A. Gadsden and A.S. Lee, Advances of the smooth variable structure filter: Square-root and two-pass formulations, *Journal of Applied Remote Sensing*, *11*(1), 2017, 15018.

[35] M. Al-Shabi and A. Elnady, Recursive smooth variable structure filter for estimation processes in direct power control scheme under balanced and unbalanced power grid, *IEEE Systems Journal*, *14*(1), 2019, 971–982.

[36] S.A. Gadsden and M. Al-Shabi, The sliding innovation filter, *IEEE Access*, *8*, 2020, 96129–96138.

[37] A. Lee, S. Gadsden, and M. AlShabi, An adaptive formulation of the sliding innovation filter, *IEEE Signal Processing Letters*, *28*, 2021, 1295–1299.

[38] M.A. AlShabi, S.A. Gadsden, M. El Haj Assad, and B. Khuwaileh, A multiple model-based sliding innovation filter, *Proc. Signal Processing, Sensor/Information Fusion, and Target Recognition XXX*, Baltimore, MD, 2021, 1175608.

[39] M. AlShabi, S. Andrew Gadsden, M. El Haj Assad, B. Khuwaileh, and S. Wilkerson, Application of the sliding innovation filter to unmanned aerial systems, *Proc. Unmanned Systems Technology XXIII*, Baltimore, MD, 2021, 117580T.

[40] S.A. Gadsden, S.R. Habibi, and T. Kirubarajan, Kalman and smooth variable structure filters for robust estimation, *IEEE Transactions on Aerospace and Electronic Systems*, *50*(2), 2014, 1038–1050.

[41] S.A. Gadsden, M. Al-Shabi, I. Arasaratnam, and S.R. Habibi, Combined cubature Kalman and smooth variable structure filtering: A robust estimation strategy, *Signal Processing*, *96*, Mar. 2014, 290–299.

[42] T.Q.S. Truong, Exploration of adaptive filters for target tracking in the presence of model uncertainty*, Proc. 6th Int. Conf. on Intelligent Sensors, Sensor Networks and Information Processing*, Brisbane, QLD, 2010, 1–6.

[43] S.A. Gadsden, Y. Song, and S.R. Habibi, Novel model-based estimators for the purposes of fault detection and diagnosis, *IEEE/ASME Transactions on Mechatronics*, *18*(4), 2013, 1237–1249.

[44] M. Esfandiari and N. Sepehri, Controller design and stability anaylysis of ouput pressure regulation in electrohydrostatic actuators, *AMSE, Journal of Dynamic Systems, Measurement, and Control*, *141*(4), 2019, 41008.

[45] A. Maddahi, W. Kinsner, and N. Sepehri, Internal leakage detection in electrohydrostatic actuators using multiscale analysis of experimental data, *IEEE Transactions on Instrumentation and Measurement*, *65*(12), 2016, 2734–2747.

[46] H.H. Afshari, S.A. Gadsden, and S.R. Habibi, Robust fault diagnosis of an electro-hydrostatic actuator using the novel optimal second-order SVSF and IMM Strategy, *International Journal of Fluid Power*, *15*(3), 2014, 181–196.

[47] S.A. Gadsden and T. Kirubarajan, Development of a variable structure-based fault detection and diagnosis strategy applied to an electromechanical system, *Proc. SPIE Signal Processing, Sensor/Information Fusion, and Target Recognition*, *XXVI*, Anaheim, CA, 2017, 102001E.

Biographies

Andrew S. Lee received the bachelor's degree in mechanical engineering from the University of Maryland at Baltimore County, and the Ph.D. degree in mechanical engineering from the University of Guelph. His specialisation is in the area of estimation theory, signal processing, and mechatronics. He is currently a Research Engineer with Northrop Grumman, Baltimore, MD, USA.

S. Andrew Gadsden received the bachelor's degree in mechanical engineering and management (business) and the Ph.D. degree in mechanical engineering from McMaster University in the area of estimation theory with applications to mechatronics and aerospace systems. He is an Associate Professor with the Department of Mechanical Engineering, McMaster University, where he is the Director of the Intelligent and Cognitive Engineering Laboratory. Before joining McMaster University, he was an Associate/Assistant Professor with the University of Guelph and an Assistant Professor with the Department of Mechanical Engineering, University of Maryland at Baltimore County, USA. He worked and continues to work with a number of colleagues in NASA, the National Institute of Standards and Technology, the U.S. Army Research Laboratory, and the U.S. Department of Agriculture. His research area includes control and estimation theory, artificial intelligence and machine learning, and cognitive systems. He is an Elected Fellow of ASME, a Senior Member of IEEE, and a Professional Engineer of Ontario. He is also a certified Project Management Professional.

Stephen A. Wilkerson (M'07) received the B.S. degree in engineering from John Hopkins University, Baltimore, MD, USA, in 1982, the M.S. degree in engineering from The George Washington University, Washington, DC, USA, in 1985, and the Ph.D. degree in mechanical engineering from Johns Hopkins University in 1990. His Ph.D. thesis was titled "A Boundary Integral Approach to Three-Dimensional Underwater Explosion Bubble Dynamics." He has an extensive experience in applied research with the U.S. government and collaborations with universities throughout the country. He continues his research and mentoring of students with the York College of Pennsylvania, York, PA, USA.

Mohammad AlShabi received the B.Sc. and M.Sc. degrees in mechatronics from the Mechanical Engineering Department, Jordan University for Science and Technology, Jordan, and the Ph.D. degree in filtering and estimation in mechatronics application from the Department of Mechanical Engineering, McMaster University, Hamilton, ON, Canada, in 2011. He is currently serving as an Associate Professor with the Department of Mechanical and Nuclear Engineering, University of Sharjah, UAE. His research areas are control, filtering, estimation, fault detection, robotics, optimization, and artificial intelligence. He helped in developing several mechatronics curriculums at M.Sc. and B.Sc. levels. He is active in research with more than 120 Scopus-indexed publications. He is an Associate Editor for IEEE Access Journal, a reviewer for more than ten Scopus-indexed journals, and a member of TPC for more than 20 conferences. He is on the steering committee for several IEEE conferences.